Pergamon

Int. J. Solids Structures Vol. 32, No. 17/18, pp. 2497–2510, 1995
Elsevier Science Ltd
Printed in Great Britain
0020-7683/95 $9.50 + .00

0020-7683(94)00279-7

CONTACT LAWS FOR CEMENTED GRAINS: IMPLICATIONS FOR GRAIN AND CEMENT FAILURE

JACK DVORKIN and HEZHU YIN
Geophysics Department, Stanford University, Stanford, CA 94305-2215, U.S.A.

(*Received* 3 *February* 1994)

Abstract—Analytical solutions are presented to predict the intergranular contact load transfer in cemented granular media where both grain material and cement are elastic. The grains can be separated, have a direct point contact, or be compacted prior to cement deposition. For all these cases contact stress distributions are obtained for normal, tangential and torsional deformation of two cemented deformable grains. An important result is that intergranular cement, even if very soft, is load-bearing. Thus cementation reduces contact stress concentration (as compared with direct Hertzian interaction). Contact stresses are maximum near the center of the contact region when the cement is soft relative to the grains, and are maximum at the periphery of the contact region when the cement is stiff. These results allow us to predict the following modes of static and dynamic failure of the grains and intergranular bonds in a particulate material. (1) Uncemented grains will tend to shatter whereas cemented grains will stay intact, and the cement will fail. (This conclusion is supported by hydrostatic loading experiments where intensive crushing of uncemented glass beads was observed at about 50 MPa, whereas grains cemented at their contacts with small amounts of epoxy stayed intact.) (2) Where intergranular cementation is present, grain failure may still be expected if the cement is strong and stiff. In this case, grain damage will be initiated at the periphery of the cement layer. (3) Yielding of a cement material that is soft (as compared with the grain material) will initiate at the center of the contact region, whereas stiff cement will yield at the periphery.

INTRODUCTION

The study of dynamic and static load transmission in granular media is important in different branches of engineering and geophysics. Artificial and natural granular materials behave as good shock attenuators and as such are used to isolate shock-sensitive instruments. Such materials can be used to protect underground facilities from explosion-associated damage. Many rocks can be treated as granular media. Understanding and quantifying shock wave propagation in rocks helps in detecting and locating nuclear explosions.

The mechanical static and dynamic characteristics of granular materials can be significantly affected by intergranular cementation. One way to understand and quantify this dependence is by studying grain-to-grain microscale interaction because in a dry granular material load is transferred mainly through contact mechanisms between neighboring particles [e.g. Oda *et al.* (1982); Shukla *et al.* (1988); Sadd *et al.* (1989)].

Recent advancements in studying the effect of intergranular cementation on the elastic and inelastic behavior of particulate materials include a numerical and experimental investigation by Bruno and Nelson (1991), an experimental study by Bernabe *et al.* (1992) and numerical (distinct element method) works by Trent (1989) and Trent and Margolin (1992). One important detail that has been missing in all these cementation-related works is a theoretical description of interparticle contact laws. Dvorkin *et al.* (1991, 1994) have examined normal and shear stress transmission between deformable particles through deformable interparticle cement bonds. Two cemented particles could be separated or have a point direct contact (Fig. 1). Three main assumptions were: (1) a thin cement layer subject to normal and shear load can be approximately treated as an elastic foundation; (2) the width of the cemented zone is small compared with the grain radius so that a grain can be treated as an elastic half-space; and (3) there is no slip between grains and at grain–cement interfaces. The first assumption has been justified by an approximate analytical solution for the normal and shear deformation of a thin smooth cement layer (Dvorkin *et*

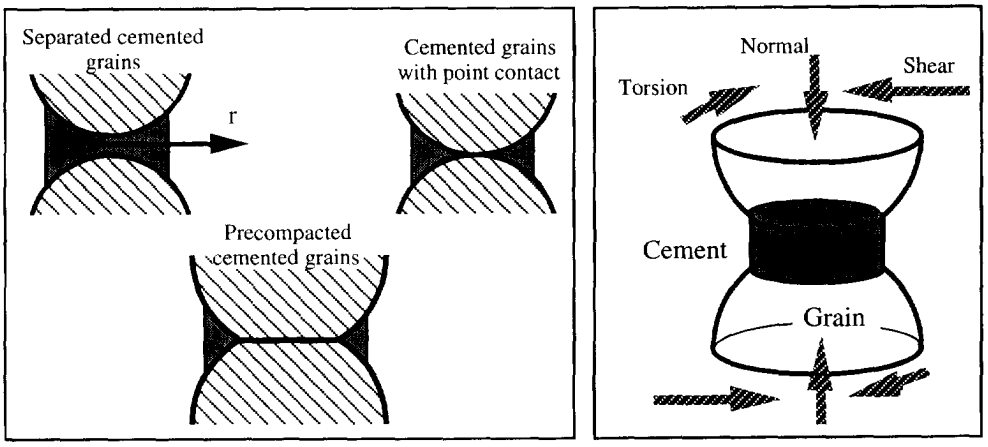

Fig. 1. Left: separated grains, grains with a point contact, and precompacted grains. Right: normal, shear, and torsional deformation of two cemented grains.

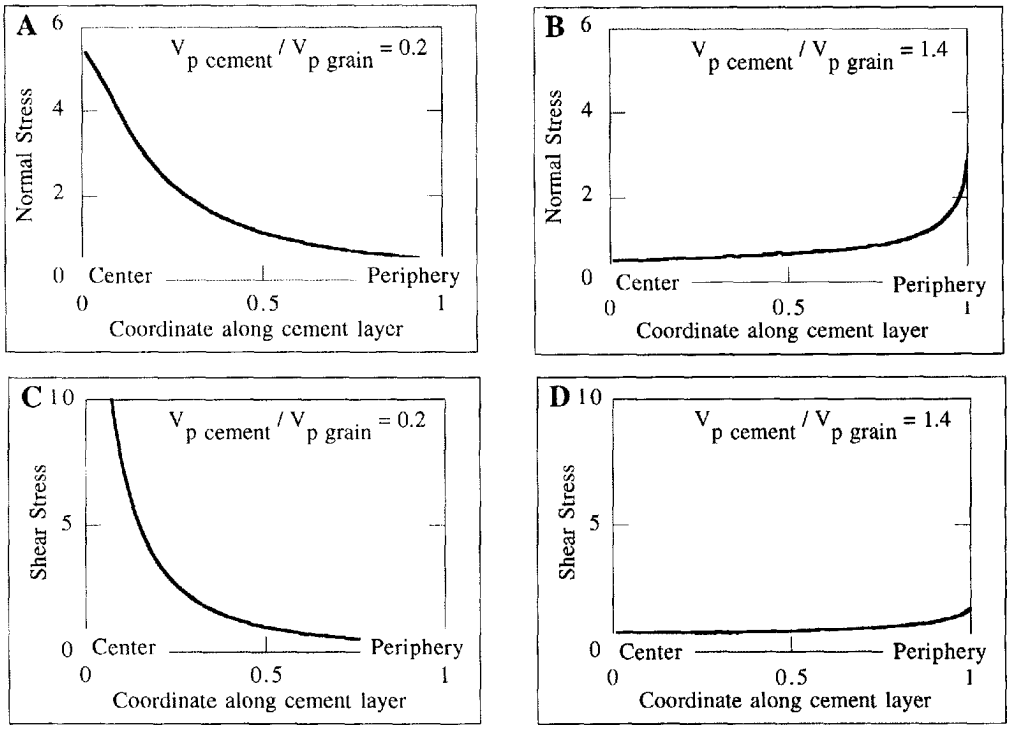

Fig. 2. Normal (A and B) and shear (C and D) stresses in the cement along the radii of the cement layers between two spherical grains with a point contact. The Poisson's ratios of both grain and cement materials are constant and equal 0.28. The stiffness of the cement varies relative to that of the grains: from very soft cement (A and C) to very stiff cement (B and D). V_p denotes compressional wave velocity in the material. The ratio of the radius of the cement layer to the grain radius is 0.33. Stresses are normalized by the average stress. The radial coordinate r (Fig. 1) is normalized by the radius of the cement layer.

al., 1991). Based on these assumptions the problem of grain–cement deformation has been reduced to an ordinary integral equation for the normal and shear stresses at the cemented interface.

The solution has revealed a peculiar pattern of normal and shear stress distribution at the cemented grain contacts: the stresses are maximum at the center of the contact region when the cement is soft relative to the grain, and are maximum at the periphery of the contact region when the cement is stiff (Fig. 2). The physical explanation of this pattern is as follows: when a soft cement layer is confined between two rigid grains, strain and stress

in it are maximum at its thinnest part—near the center of contact. When the cement is stiff relative to the grain material, its action on the grain is close to that of a rigid punch penetrating an elastic half-space [e.g. Johnson (1992)]. In this case stress concentration is expected at the periphery of the punch.

The macroscopic stiffness of a cemented system increases with the increasing radius of the cement layer and with its increasing stiffness. The former factor is the most important: the small increase of the cementation content results in significant growth of a contact zone between two contacting grains and, because the cement is load-bearing, dramatically increases the stiffness of a two-grain system and thus the macroscopic stiffness of a cemented particulate material. This conclusion holds even if the cement is relatively soft.

In this paper we concentrate on the description of normal, shear and torsional stress transmission between two elastic grains that were initially precompacted by a normal force to develop a finite (Hertzian) direct contact area. Afterwards cement was deposited around the initial contact zone (Fig. 1). Our analytical solutions have been obtained under the same assumptions as in the uncompacted case. The results show that in soft cement, normal and shear stresses developed due to the continuing deformation of two grains are maximum at the periphery of the initial contact zone between two grains. These stresses reduce towards the periphery of the cement layer. However, in stiff cement, contact stresses are maximum at the periphery of the cement layer.

Below, we give solutions to the problems of normal and shear deformation of two precompacted cemented spherical grains. Similar solutions for two-dimensional grains (cylinders) are given in Appendix A. Torsional deformation of two spherical cemented grains (both uncompacted and precompacted cases) is explored in Appendix B. The theoretical results are compared with our experimental data.

We also discuss the implications of the obtained solutions for the failure of cemented granular materials.

NORMAL AND SHEAR DEFORMATION OF TWO PRECOMPACTED GRAINS

Precompacted grains

Consider two identical elastic spherical grains of radius R that are normally pressed together by force P_H to form a circular contact area of radius a. Then

$$a = \sqrt[3]{\left(\frac{3P_H R(1-\nu)}{8G}\right)}, \tag{1}$$

where G and ν are the grain shear modulus and Poisson's ratio, respectively (e.g. Johnson (1992)]. This intergranular force P_H can be easily calculated from the hydrostatic pressure P_0 acting at a random pack of identical spherical grains:

$$P_H = \frac{4\pi R^2 P_0}{C(1-\phi)}, \tag{2}$$

where C is the average number of contacts per grain (about nine) and ϕ is the porosity of the pack (about 36%).

From Hertz's solution, the initial distribution of normal stresses p_H on the surface of the precompacted grains is:

$$p_H = -\frac{4G}{\pi R(1-\nu)}\sqrt{(a^2-r^2)}, r \leqslant a;$$

$$p_H = 0, r > a. \tag{3}$$

The corresponding initial displacements v_H of the grain surface are:

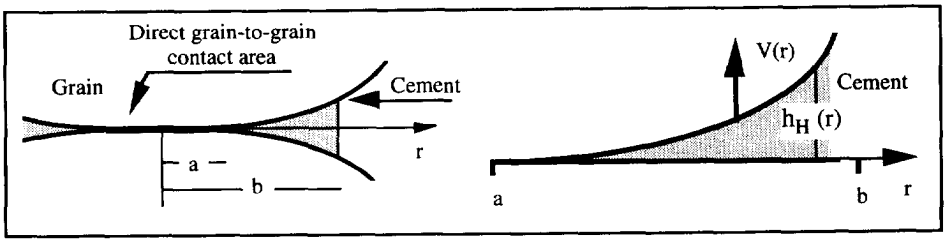

Fig. 3. Left: contact area between two precompacted cemented grains with cement added after compaction. Right: cement layer, its initial thickness and its displacements.

$$v_H(r) = \frac{a^2}{R} - \frac{r^2}{2R}, 0 \leqslant r \leqslant a;$$

$$v_H(r) = \frac{1}{\pi R}\left[(2a^2 - r^2)\arcsin\left(\frac{a}{r}\right) + ar\sqrt{\left(1 - \frac{a^2}{r^2}\right)}\right], \quad a < r \leqslant b. \tag{4}$$

After the initial compaction, elastic cement is uniformly added around the direct grain contact zone to increase the radius of the contact area to b (Fig. 3). It follows from eqns (4) that the half-thickness of the undeformed cement layer between two precompacted spherical grains is:

$$h_H(r) = \frac{a^2}{\pi R}\left[\left(\frac{r^2}{a^2} - 2\right)\arctan\sqrt{\left(\frac{r^2}{a^2} - 1\right)} + \sqrt{\left(\frac{r^2}{a^2} - 1\right)}\right], a \leqslant r \leqslant b. \tag{5}$$

Normal deformation

Consider now additional normal loading of the grains with force ΔP that produces additional displacement δ of each grain's center towards their contact zone. The resulting total normal displacements $v(r)$ of the grain surface within the area of the initial direct contact are:

$$v(r) = \delta - \frac{r^2}{2R}, \quad 0 < r \leqslant a. \tag{6}$$

Within the cemented zone, $a < r \leqslant b$, the total normal displacements of the grain surface $v(r)$ are related to the normal displacements of the cement as:

$$V(r) = v(r) - v_H(r) - \delta + \frac{a^2}{R}, \tag{7}$$

where $V(r)$ is the normal displacement of the cement surface (at the cement–grain interface) relative to the median plane of the cement layer (Fig. 3).

By treating the cement layer as an elastic foundation, we have the following expression for normal stresses $p(r)$ at the cement–grain interface:

$$p(r) = -\frac{2G_c(1 - \nu_c)}{1 - 2\nu_c}\frac{V(r)}{h_H(r)}, \quad a < r \leqslant b, \tag{8}$$

where G_c and ν_c are the cement's shear modulus and Poisson's ratio, respectively.

Finally, treating the grain as an elastic half-space, we have the following expression that relates normal stresses $p(r)$ to normal displacements $v(r)$ of the grain's surface (Timoshenko and Goodier, 1970):

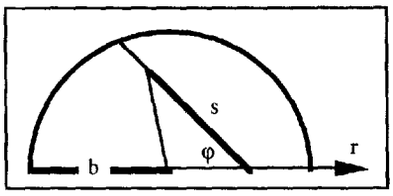

Fig. 4. Domain of integration in eqn (9).

$$v(r) = \frac{(1-\nu)}{\pi G}\int_0^{\pi} d\varphi \int_0^{r\cos\varphi+\sqrt{(b^2-r^2\sin^2\varphi)}} p[\sqrt{(r^2+s^2-2rs\cos\varphi)}]\,ds, \tag{9}$$

where the integration is inside the circle $|r| \leqslant b$ (Fig. 4).

Now we combine eqns (6)–(9) to obtain the following integral equation for normal stress $p(r)$:

$$v(r) = \frac{(1-\nu)}{\pi G}\int_0^{\pi} d\varphi \int_0^{r\cos\varphi+\sqrt{(b^2-r^2\sin^2\varphi)}} p[\sqrt{(r^2+s^2-2rs\cos\varphi)}]\,ds$$

$$= \begin{cases} \delta - \dfrac{r^2}{2R}, & 0 \leqslant r \leqslant a; \\ v_H(r) + \delta - \dfrac{a^2}{R} - \dfrac{1-2\nu_c}{2G_c(1-\nu_c)} p(r) h_H(r), & a < r \leqslant b. \end{cases} \tag{10}$$

Let us present the normal stress $p(r)$ as the sum of the initial Hertzian stress $p_H(r)$ and the additional normal stress $f(r)$:

$$p(r) = p_H(r) + f(r). \tag{11}$$

It follows then from eqns (4) and (9)–(11) that

$$\frac{(1-\nu)}{\pi G}\int_0^{\pi} d\varphi \int_0^{r\cos\varphi+\sqrt{(b^2-r^2\sin^2\varphi)}} f[\sqrt{(r^2+s^2-2rs\cos\varphi)}]\,ds$$

$$= \begin{cases} \delta - \dfrac{a^2}{2R}, & 0 \leqslant r \leqslant a; \\ \delta - \dfrac{a^2}{R} - \dfrac{1-2\nu_c}{2G_c(1-\nu_c)} f(r) h_H(r), & a < r \leqslant b. \end{cases} \tag{12}$$

This last equation can be easily solved using the numerical quadrature method [e.g. Delves and Mohamed (1985)].

The constant δ can be found from the resulting force ΔP:

$$\Delta P = \int_0^b f(r) 2\pi r\,dr. \tag{13}$$

Shear deformation

Our treatment of the shear deformation of two cemented grains is analogous to that of the normal deformation: we assume that after cement deposition a tangential force Q is exerted on the system to produce the tangential displacement τ of each grain's center relative to the contact zone. The resulting tangential displacements $u(r)$ of the grain surface within the area of the initial direct contact are:

$$u(r) = \tau, 0 < r \leqslant a. \tag{14}$$

Within the cemented zone, $a < r \leqslant b$, the tangential displacements of the grain surface $u(r)$ are related to the tangential displacements of the cement as:

$$U(r) = u(r) - \tau, \tag{15}$$

where $U(r)$ is the displacement of the cement surface (at the cement–grain interface) relative to the median plane of the cement layer.

By treating the cement layer as an elastic foundation in shear, we have the following expression for tangential stresses $q(r)$ at the cement–grain interface:

$$q(r) = -G_c \frac{U(r)}{h_H(r)}, a < r \leqslant b. \tag{16}$$

Now treating the grain as an elastic half-space, we have the following approximate expression that relates shear stresses $q(r)$ to tangential displacements $u(r)$ of the grain's surface (Dvorkin *et al.*, 1994):

$$u(r) = \frac{1}{\pi G} \int_0^{\pi} d\varphi \int_0^{r\cos\varphi + \sqrt{(b^2 - r^2 \sin^2\varphi)}} q[\sqrt{(r^2 + s^2 - 2rs\cos\varphi)}](1 - \nu \sin^2\varphi)\, ds, \tag{17}$$

where the integration is inside the circle $|r| \leqslant b$ (Fig. 4).

Finally, we combine eqns (14)–(17) to obtain the following integral equation for shear stress $q(r)$:

$$u(r) = \frac{1}{\pi G} \int_0^{\pi} d\varphi \int_0^{r\cos\varphi + \sqrt{(b^2 - r^2 \sin^2\varphi)}} q[\sqrt{(r^2 + s^2 - 2rs\cos\varphi)}](1 - \nu \sin^2\varphi)\, ds$$

$$= \begin{cases} \tau, & 0 \leqslant r \leqslant a; \\ \tau - \dfrac{1}{G_c} q(r) h_H(r), & a < r \leqslant b. \end{cases} \tag{18}$$

Again, this integral equation can be easily solved using the numerical quadrature method.

The constant τ can be found from the resulting force Q:

$$Q = \int_0^b q(r) 2\pi r\, dr. \tag{19}$$

Contact stresses

Normal stresses in the contact zone of two precompacted grains are given in Fig. 5.

The ratio of the cement radius b to the grain radius R was 0.7, the radius a of the initial zone of direct grain contact was 0.105 of R (0.15 of b). The elastic moduli of the grains were constant and equal to those of glass (bulk modulus 49.9 GPa and shear modulus 26.2 GPa). The bulk and shear moduli of the cement varied from 1.7 and 0.5 GPa, respectively, to 170.0 and 50.0 GPa. In the second example (6.8 and 2.0 GPa) the elastic moduli of the cement are identical to those of epoxy.

When the cement is relatively soft, we observe the concentration of the additional normal contact stresses at the periphery of the direct grain contact zone ($r = a$). The physical meaning of this effect is: in the soft cement layer stresses are maximum at its thinnest part—near its inner boundary ($r \to a, r > a$). In the direct grain contact region we have the condition of a constant additional displacement δ—analogous to that on the face of a rigid punch penetrating an elastic half-space. This is the reason for the additional

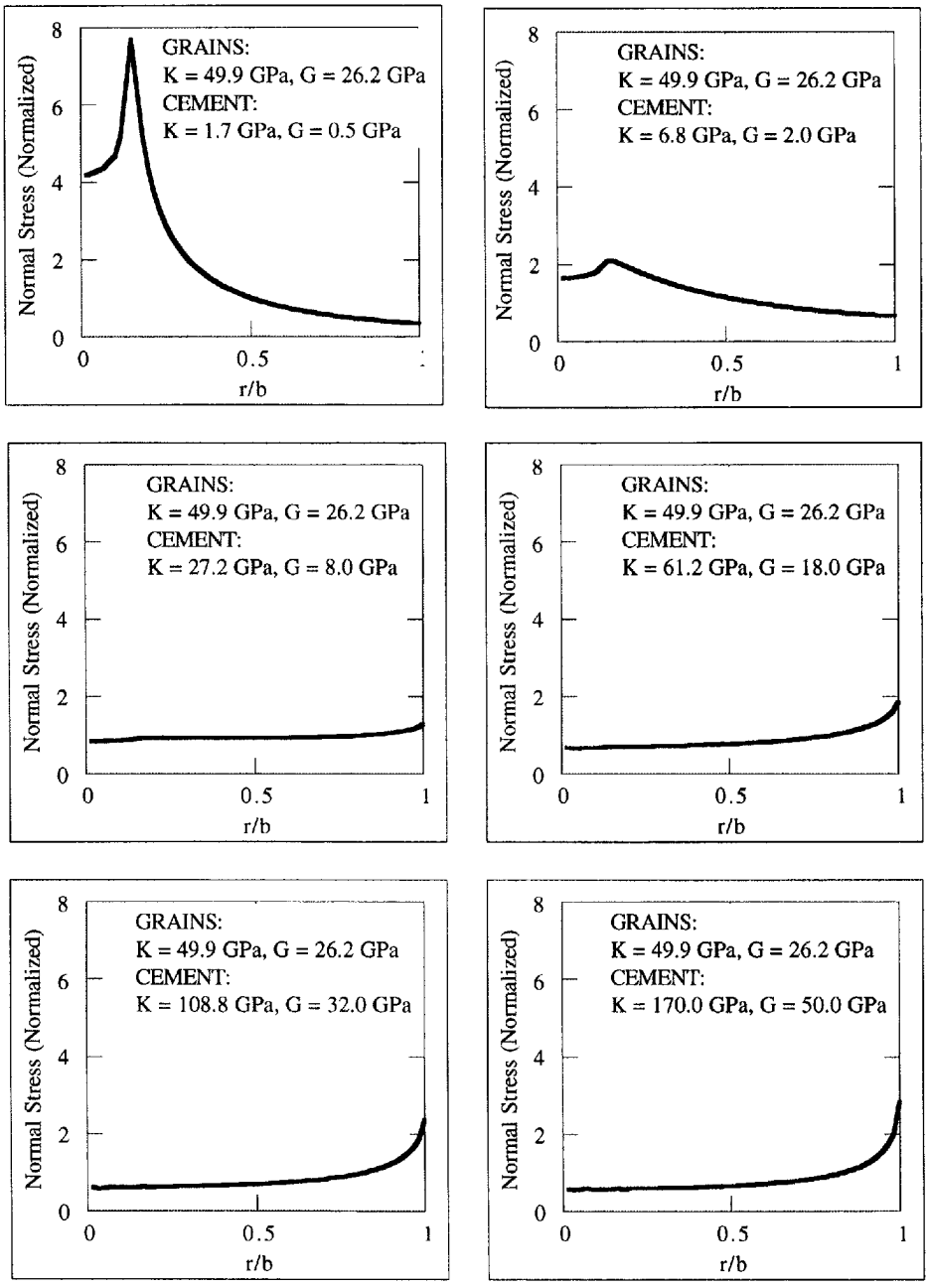

Fig. 5. Additional normal stresses $f(r)$ along the radii of cement layers for varying relative rigidity of the cement and grain materials. Stresses are normalized by the average additional stress. The horizontal axis is the normalized distance along the radius of the cement layer.

contact stress concentration on the direct contact side ($r \to a, r < a$) of the contact region $0 \leqslant r \leqslant b$.

As the cement becomes stiffer, its action on the grain approaches that of a rigid punch of radius b. Therefore, we observe stress concentration on the periphery of the cement layer at $r = b$.

Shear stresses for the six above cases are given in Fig. 6. The patterns of stress distribution and their physical meaning are similar to those observed for normal stresses. It is important to notice that in this case we have used the no-slip condition in the direct grain-to-grain contact zone. Clearly, this condition is not valid if shear stresses are high and slip does occur. However, we justify this approximation by the fact that for small tangential forces exerted on contacting bodies, stress distributions that are produced from

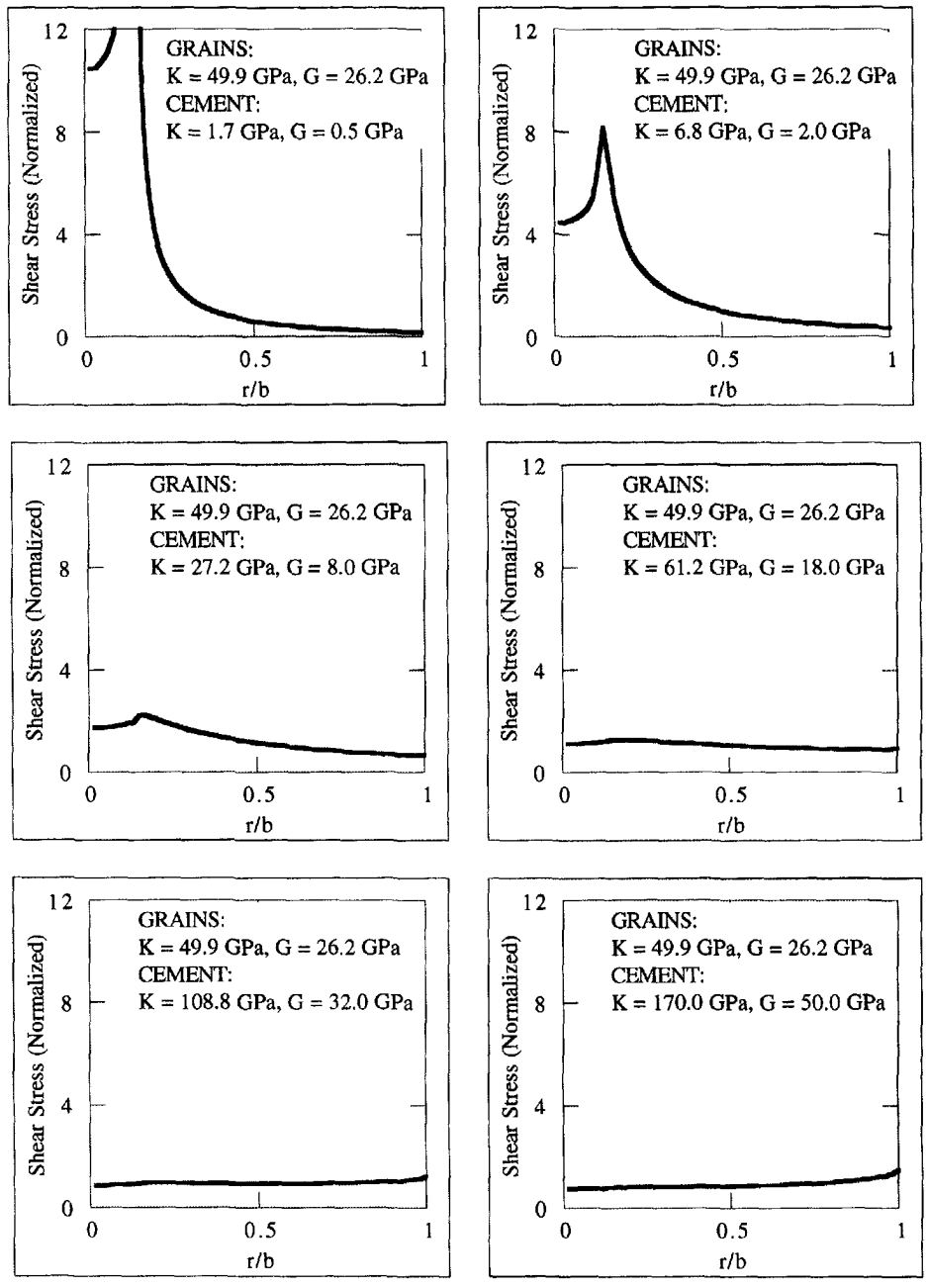

Fig. 6. Shear stresses $q(r)$ along the radii of cement layers for varying relative rigidity of the cement and grain materials. Stresses are normalized by the average shear stress. The horizontal axis is the normalized distance along the radius of the cement layer.

the no-slip solutions are fairly close to those produced from the partial-slip solutions [see examples in Johnson (1992)].

EXPERIMENT

Our experiment has been conducted on hydrostatically precompacted glass beads cemented with epoxy. The cemented samples were prepared by mixing glass beads (0.2–0.3 mm in diameter) with a given volume of epoxy (10, 25, 50 and 100% of the pore space volume). They were compacted at 20 MPa prior to epoxy solidification. Compressional (V_p) and shear (V_s) wave velocities have been measured at 1 MHz frequency using the pulse transmission technique.

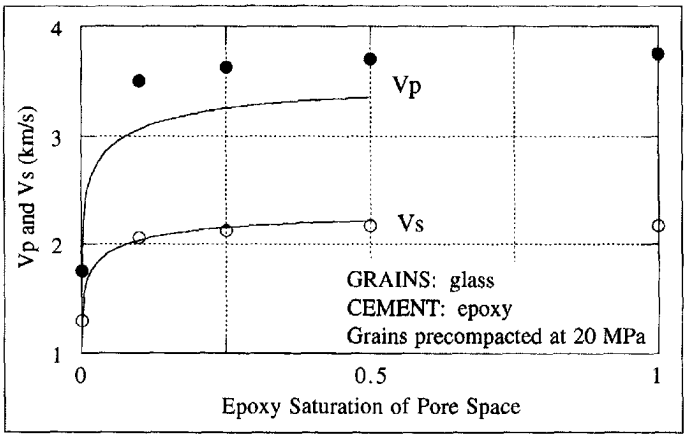

Fig. 7. Experimental and theoretical results on precompacted epoxy-cemented glass beads. Circles show experimental points, solid lines are theoretical predictions.

The above-derived contact laws for the normal and shear deformation of two precompacted cemented grains have been used to calculate the effective bulk and shear moduli of a random packing of identical elastic spheres. These theoretical predictions are compared with the experimental results in Fig. 7. The agreement between the theory and the experiments is within 15% accuracy.

IMPLICATIONS FOR GRAIN AND CEMENT FAILURE

One important result following from the above-derived grain–cement–grain contact laws is that intergranular cement, even if very soft, is load-bearing. Thus cementation reduces contact stress concentration (compared with direct Hertzian interaction). As a result, even small amounts of relatively soft cement may prevent grain failure: uncemented grains will tend to shatter whereas cemented grains will stay intact and the cement will fail. This conclusion has been supported by hydrostatic loading experiments where intensive crushing of uncemented glass beads was observed at about 50 MPa, whereas grains cemented at their contacts with small amounts of epoxy (10% of the pore space volume) stayed intact (Fig. 8). The observed effect follows from our theory of cemented granular

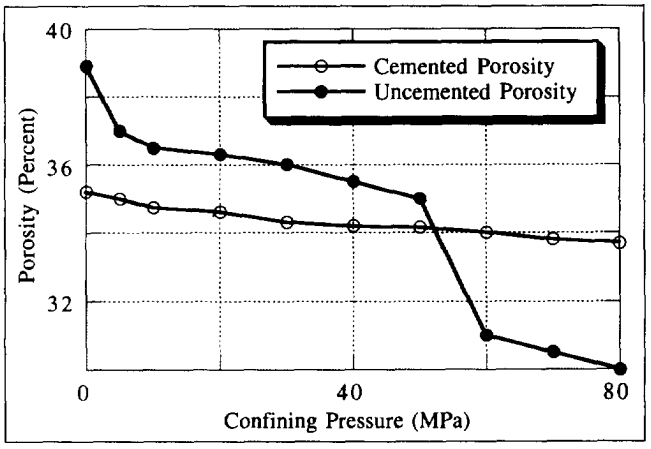

Fig. 8. Porosity versus hydrostatic confining pressure in water-saturated randomly packed glass beads that were (a) uncemented and (b) cemented by epoxy at their contacts (Yin and Dvorkin, 1994). Porosity was measured by the volume of expelled fluid. In the uncemented case, a sharp porosity decrease is observed at about 50 MPa. The decrease is associated with the crushing of grains. The cemented grains (the volume of the epoxy accounted for only 10% of the pore space) did not crush. The photos showed that in the latter case, the grains stayed intact with the failure being localized within the epoxy.

materials: stress concentration is high at the contacts of uncemented grains, whereas even small amounts of relatively soft cement result in a more uniform stress distribution over a larger contact area. The total force transmitted between two grains must, of course, remain the same in the cemented and uncemented cases; however, the stresses at the cemented interface decrease dramatically compared with the Hertzian contact case.

The contact stress distributions as obtained, imply the following modes of static and dynamic failure of the grains and intergranular bonds in a particulate material: (1) uncemented grains will tend to fail whereas cemented grains will stay intact, and the cement will fail; (2) where intergranular cementation is present, grain failure may still be expected if the cement is strong and stiff—in this case, grain damage will be initiated at the periphery of the cement layer; (3) yielding of a cement material that is soft (compared with the grain material) will initiate at the center of the contact region, whereas stiff cement will yield at the periphery.

CONCLUSIONS

All the solutions presented in this paper have been applied to the interaction of two circular grains. Note that the contact law solutions obtained are more general and can be applied to cemented elastic grains with arbitrarily-shaped contact surfaces as long as the underlying assumptions are valid. Specifically, the cement layer has to be thin and small compared with a grain, and in addition contacting grain surfaces have to be smooth, so that the elastic foundation approximation is valid. The shape of grain surfaces will affect the thickness of the cement layer, and the initial stress distribution at the direct contact area of precompacted grains.

In the example presented in Fig. 7 we have used formulas for the effective bulk and shear moduli of a random packing of identical spherical grains as given by Digby (1981) and Winkler (1983). Again, our contact laws can be used to describe the effective properties of more complicated arrangements of cemented grains. Specifically, these contact laws can be plugged into sophisticated numerical schemes (e.g. the Distinct Element Method).

One important assumption that has been used in treating the problems of shear and torsional deformation of precompacted cemented grains is the no-slip condition in the direct grain-to-grain contact zone. This assumption is valid only if stresses are small, so that stress distributions obtained under the no-slip assumption are close to those obtained by considering the relative sliding of contacting grains [see examples in Johnson (1992)]. At the same time, the computed shear stress distributions shown in Fig. 6 indicate that the sliding will initiate at the periphery of the direct grain-to-grain contact area only if the cement is very soft compared with the grain material. In most cases, we do not expect to encounter high stress concentration and sliding in the mentioned area.

The solutions presented can describe the dynamic interaction of cemented grains only if the quasi-static approximation is valid, i.e. the wavelength is significantly larger than the characteristic microscopic dimension (the grain radius). This was the case in the ultrasonic pulse transmission experiment described above: the wavelength was approximately 10 times the average grain diameter. These solutions can also be applied to describing shock wave propagation in a particulate medium if the length of the pulse is much larger than the grain radius.

Acknowledgement—This work was supported by the U.S. Air Force Office of Scientific Research, Project 2302C.

REFERENCES

Bernabe, Y., Fryer, D. T. and Hayes, J. A. (1992). The effect of cement on the strength of granular rocks. *Geophys. Res. Lett.* **19,** 1511–1514.

Bruno, M. S. and Nelson, R. B. (1991). Microstructural analysis of the inelastic behavior of sedimentary rock. *Mech. Mater.* **12,** 95–118.

Delves, L. M. and Mohamed, J. L. (1985). *Computational Methods for Integral Equations*. Cambridge University Press, Cambridge.

Digby, P. J. (1981). The effective elastic moduli of porous granular rocks. *J. Appl. Mech.* **48,** 803–808.

Dvorkin, J., Mavko, G. and Nur, A. (1991). The effect of cementation on the elastic properties of granular material. *Mech. Mater.* **12,** 207–218.
Dvorkin, J., Nur, A. and Yin, H. (1994). Effective properties of cemented granular materials. *Mech. Mater.* **18,** 351–366.
Johnson, K. L. (1992). *Contact Mechanics.* Cambridge University Press, Cambridge.
Oda, M., Nemat-Nasser, S., and Mehrabadi, M. M. (1982). A statistical study of fabric in a random assembly of spherical granules. *Int. J. Num. Anal. Meth. Geomech.* **6,** 77–94.
Sadd, M. H., Shukla, A. and Mei, H. (1989). Computational and experimental modeling of wave propagation in granular materials. In *Proceedings of the 4th International Conference on Computational Methods and Experimental Measurements*, Capri, Italy, pp. 325–334.
Shukla, A., Zhu, C. Y. and Sadd, M. H. (1988). Angular dependence of dynamic load due to explosive loading in two dimensional granular aggregates. *J. Strain Anal.* **23,** 121–127.
Timoshenko, S. P. and Goodier, J. N. (1970). *Theory of Elasticity.* McGraw-Hill, New York.
Trent, B. C. (1989). Numerical simulation of wave propagation through cemented granular material. In *AMD—101, Wave Propagation in Granular Media* (edited by D. Karamanlidis and R. B. Stout), pp. 9–15.
Trent, B. C. and Margolin, L. G. (1992). A numerical laboratory for granular solids. *Engng Comp.* **9,** 191–197.
Yin, H. and Dvorkin, J. (1994). Strength of cemented grains. *Geophys. Res. Lett.* **21,** 903–906.
Winkler, K. W. (1983). Contact stiffness in granular porous materials: comparison between theory and experiment. *Geophys. Res. Lett.* **10,** 1073–1076.

APPENDIX A: TWO PRECOMPACTED CYLINDERS

Precompaction

Consider two identical elastic circular cylinders (plane strain) of radius R that are normally pressed together by force P_H to form a contact area of half-width a. Then (Johnson, 1992)

$$a = \sqrt{\left(\frac{2P_H R(1-\nu)}{\pi G}\right)}. \tag{A1}$$

The initial distribution of normal stresses p_H on the surface of the precompacted cylinders is:

$$p_H = \frac{G}{R(1-\nu)}\sqrt{(a^2-r^2)}, \quad |x| \leqslant a;$$
$$p_H = 0, |x| > a. \tag{A2}$$

Here x is the coordinate along the median line of the cement layer in the plane perpendicular to the cylinder's axis, analogous to the r coordinate in the three-dimensional case.

By treating the cylinder as an elastic half-plane, we have the following expression for the initial normal displacements $v_H(r)$ of the cylinder's surface from normal stresses $p_H(r)$ (Johnson, 1992):

$$v_H(x) = -\frac{1-\nu}{\pi G}\int_{-b}^{b} p_H(s)\ln|x-s|\,ds + \text{const.} \tag{A3}$$

After the initial compaction, cement is uniformly added around the direct contact zone to increase the half-width of the contact area to b. It follows from eqn (A3) that the half-thickness of the undeformed cement layer between two precompacted circular cylinders is:

$$h_H(x) = \frac{x^2-a^2}{2R} - \frac{1}{\pi R}\int_{-a}^{a}\sqrt{(a^2-s^2)}\ln\left|\frac{x-s}{a-s}\right|ds + \text{const}, \quad a < |x| \leqslant b. \tag{A4}$$

Normal deformation

Consider now additional normal loading of the cylinders with force ΔP. The resulting total normal displacements $v(x)$ of the cylinder surface within the area of the initial direct contact are:

$$v(x) - v(a) = \frac{a^2-x^2}{2R}, \quad |x| \leqslant a. \tag{A5}$$

Within the cemented zone, $a < |x| \leqslant b$, the total normal displacements of the grain surface $v(x)$ are related to the normal displacements of the cement as:

$$V(x) = v(x) - v(a) - [v_H(x) - v_H(a)], \quad a < |x| \leqslant b, \tag{A6}$$

where $V(r)$ is the normal displacement of the cement surface (at the cement–cylinder interface) relative to the median line of the cement layer.

By treating the cement layer as an elastic foundation, we have the following expression for normal stresses $p(x)$ at the cement–grain interface:

$$p(x) = -\frac{2G_c(1-\nu_c)}{1-2\nu_c}\frac{V(x)}{h_H(x)}, \quad a < |x| \leqslant b. \tag{A7}$$

Equation (A3) now takes the following form:

$$v(x) = -\frac{1-\nu}{\pi G}\int_{-b}^{b} p(s)\ln|x-s|\,ds + \text{const}. \tag{A8}$$

Now we combine eqns (A5)-(A8) to obtain the following integral equation for normal stress $p(x)$:

$$v(x)-v(a) = -\frac{1-\nu}{\pi G}\left[\int_{-b}^{b} p(s)\ln|x-s|\,ds - \int_{-b}^{b} p(s)\ln|x-s|\,ds\right]$$

$$= \begin{cases} \dfrac{a^2-x^2}{2R}, & |x| \leqslant a; \\ v_H(x)-v_H(a)-\dfrac{1-2\nu_c}{2G_c(1-\nu_c)}p(x)h_H(x), & a < |x| \leqslant b. \end{cases} \tag{A9}$$

Let us now present the normal stress $p(x)$ as the sum of the initial Hertzian stress $p_H(x)$ and the additional normal stress $f(x)$:

$$p(x) = p_H(x) + f(x). \tag{A10}$$

It follows then from eqns (A2), (A3), (A9), and (A10) that

$$\int_{-b}^{b} f(s)\ln|x-s|\,ds + \text{const} = \begin{cases} 0, & |x| \leqslant a; \\ \dfrac{\pi G}{1-\nu}\dfrac{1-2\nu_c}{2G_c(1-\nu_c)}f(x)h_H(x), & a < |x| \leqslant b. \end{cases} \tag{A11}$$

This last equation can be solved using the numerical quadrature method.

The constant in the left-hand part of eqn (A11) can be found from the resulting force ΔP:

$$\Delta P = \int_{-b}^{b} f(x)\,dx. \tag{A12}$$

Shear deformation

In the two-dimensional case under consideration, the treatment of the shear deformation of two cemented grains is identical to that of the normal deformation: eqn (A8) is replaced by:

$$u(x) = -\frac{1-\nu}{\pi G}\int_{-b}^{b} q(s)\ln|x-s|\,ds + \text{const}; \tag{A13}$$

eqn (A5) is replaced by

$$u(x)-u(a) = 0, \quad |x| \leqslant a; \tag{A14}$$

eqn (A6) is replaced by

$$U(x) = u(x)-u(a), \quad a < |x| \leqslant b; \tag{A15}$$

and eqn (A7) is replaced by

$$q(x) = -G_c\frac{U(x)}{h_H(x)}, \quad a < |x| \leqslant b. \tag{A16}$$

The definitions of the tangential displacements $u(x)$ of the cylinder's surface, tangential displacements $U(x)$ of the cement, and shear stresses $q(x)$ in contact zone are the same as in the spherical case. Again, as in the spherical case, we assume the no-slip condition in the direct contact zone. This assumption is valid if shear stresses are small.

Similar to the case of normal deformation, we arrive at the following integral equation for stresses $q(x)$:

$$\int_{-b}^{b} q(s)\ln|x-s|\,ds + \text{const} = \begin{cases} 0, & |x| \leqslant a; \\ \dfrac{\pi G}{(1-\nu)G_c}q(x)h_H(x), & a < |x| \leqslant b, \end{cases} \tag{A17}$$

where the constant in the left-hand part of equation can be found from the resulting shear force Q:

$$Q = \int_{-b}^{b} q(x)\,\mathrm{d}x. \tag{A18}$$

Normal and shear stress distributions in this two-dimensional case are qualitatively similar to those obtained for two precompacted spheres.

APPENDIX B: TORSIONAL DEFORMATION OF TWO SPHERICAL GRAINS

Uncompacted grains

Consider a twisting moment M applied to the system of two cemented spherical grains (Fig. 1). Shear stress components $q(r)$ acting on the grain–cement interface are axisymmetrical, and the only non-zero displacement of the grain surface $u(r)$ is perpendicular to the polar radius r (Fig. B1).

The displacements $u(r)$ are related to stresses $q(r)$ as (Johnson, 1992):

$$u(r) = \frac{1}{\pi G}\int_0^{\pi} \mathrm{d}\varphi \int_0^{r\cos\varphi + \sqrt{(a^2 - r^2\sin^2\varphi)}} \frac{q[\sqrt{(r^2+s^2-2rs\cos\varphi)}]}{\sqrt{(r^2+s^2-2rs\cos\varphi)}}(r - s\cos\varphi)\,\mathrm{d}s, \tag{B1}$$

where integration is inside the circle $|r| \leqslant a$ in the plane of contact (see Fig. 4).

The tangential displacement of the grain surface $u(r)$ and the tangential displacement of the cement layer surface relative to its median plane $U(r)$ are related to the respective angles of rotation $\beta(r)$ and $B(r)$ as:

$$u(r) = r\beta(r),\ U(r) = rB(r). \tag{B2}$$

The condition of displacement compatibility between the grain and the cement surface is:

$$\beta(r) = B(r) + \gamma, \tag{B3}$$

where γ represents the grain's rigid rotation.

Treating the cement layer as an elastic foundation in torsion, we have the following relation between stress $q(r)$ and angle $B(r)$:

$$q(r) = -G_c\frac{U(r)}{h(r)} = -G_c\frac{rB(r)}{h(r)}, \tag{B4}$$

where $h(r)$ is the half-width of the cement layer. For a cement layer between two spheres:

$$h(r) = R\left[\varepsilon + \frac{1}{2}\left(\frac{r}{R}\right)^2\right],\ \varepsilon = \frac{h_0}{R}, \tag{B5}$$

where h_0 is the minimum half-separation between the spheres.

Finally, eqns (B1)–(B5) yield the following integral equation for $B(r)$:

$$r[\gamma + B(r)] = -\frac{G_c}{\pi G}\int_0^{\pi} \mathrm{d}\varphi \int_0^{r\cos\varphi + \sqrt{(a^2 - r^2\sin^2\varphi)}} \frac{B[\sqrt{(r^2+s^2-2rs\cos\varphi)}](r - s\cos\varphi)}{R\left[\varepsilon + \frac{1}{2}\left(\frac{r^2}{R^2} + \frac{s^2}{R^2} - 2\frac{rs}{R^2}\cos\varphi\right)\right]}\,\mathrm{d}s. \tag{B6}$$

The constant γ in eqn (B6) can be found from the resulting twisting moment M:

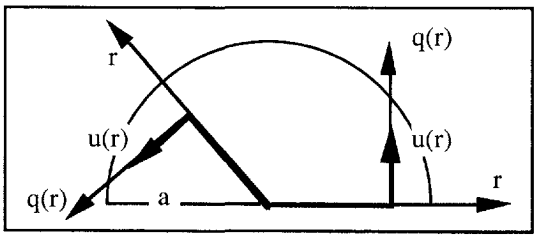

Fig. B1. Torsional displacements and shear stresses in the plane of grain–cement–grain contact. The problem under consideration is treated in a linear approximation, so we assume the contact zone is planar.

$$M = -2\pi G_c \int_0^a \frac{B(r)r^3}{R\left(\varepsilon + \dfrac{r^2}{2R^2}\right)}\,\mathrm{d}r. \tag{B7}$$

The resulting distributions of the twisting shear stresses along the radius of a cement layer are qualitatively similar to those shown in Fig. 2.

Precompacted grains

The treatment of this problem is analogous to that used in the problems of normal and shear deformation of two precompacted grains. The resulting integral equation for the twisting shear stresses $q(r)$ in the contact zone is:

$$\frac{1}{\pi G}\int_0^{\pi} \mathrm{d}\varphi \int_0^{\sqrt{(r\cos\varphi+\sqrt{b^2-r^2\sin^2\varphi})^2+r^2\sin^2\varphi}} \frac{q[\sqrt{(r^2+s^2-2rs\cos\varphi)}](r-s\cos\varphi)}{\sqrt{(r^2+s^2-2rs\cos\varphi)}}\,\mathrm{d}s = \begin{cases} \gamma r, & r \leqslant a; \\ \gamma r - \dfrac{q(r)h_H(r)}{G_c}, & a < r \leqslant b. \end{cases} \tag{B8}$$

The constant γ here can be found from the resulting twisting moment:

$$M = 2\pi \int_0^b q(r)r^2\,\mathrm{d}r. \tag{B9}$$

The computed distributions of twisting shear stresses are similar to those shown in Fig. 6.

This solution uses the no-slip condition in the direct grain–grain contact zone. The assumption is valid if shear stresses are small.